J Solid State Electrochem (2011) 15:147–152
DOI 10.1007/s10008-010-1079-8

ORIGINAL PAPER

Anode performance of Mn-doped ceria–ScSZ for solid oxide fuel cell

Guoqiang Cai · Renzhu Liu · Chunhua Zhao · Junliang Li · Shaorong Wang · Tinglian Wen

Received: 4 February 2010 / Revised: 11 April 2010 / Accepted: 14 April 2010 / Published online: 4 May 2010

Abstract The 70 wt.% Mn-doped CeO_2 (MDC)-30 wt.% Scandia-stabilized zirconia (ScSZ) composites are evaluated as anode materials for solid oxide fuel cells (SOFCs) in terms of chemical compatibility, thermal expansion coefficient, electrical conductivity, and fuel cell performance in H_2 and CH_4. The conductivity of MDC10 (10 mol.% Mn-doping), MDC20, and CeO_2 are 4.12, 2.70, and 1.94 $S cm^{-1}$ in H_2 at 900 °C. With 10 mol.% Mn-doping, the fuel cells performances improve from 166 to 318 mW cm^{-2} in H_2 at 900 °C. The cell with MDC10–ScSZ anode exhibits a better performance than the one with MDC20–ScSZ in CH_4, the maximum power density increases from 179 to 262 mW cm^{-2}. Electrochemical impedance spectra indicate that the Mn doping into CeO_2 can reduce the ohmic and polarization resistance, thus leading to a higher performance. The results demonstrate the potential ability of MDC10–ScSZ composite to be used as SOFCs anode.

Keywords Solid oxide fuel cell · Manganese doped-ceria · Anode · Scandia-stabilized zirconia · Methane

Introduction

As a promising technology for high efficiency power generation system, solid oxide fuel cells (SOFCs) offer a clean and electrochemical way to convert chemical energy of fossil fuel into electrical power directly [1]. Directly utilizing hydrocarbon fuels to replace hydrogen is the key issue to accelerate the commercialization of SOFCs [2], since hydrogen is more expensive than hydrocarbon; and it has many problems with mass storage and transportation. However, the state-of-the-art Ni-based cermet anode cannot be used for hydrocarbon because Ni is a good catalyst for the hydrocarbon cracking reaction that will lead to carbon deposition [3–10]. Therefore, it is necessary to develop an alternative anode material to resolve the problems with Ni-YSZ (yttria-stabilized zirconia).

Ceria-based mixed conductors [11] can realize the direct utilization of hydrocarbon fuels because they have a remarkable resistance to carbon deposition [12–16]. It has been reported that sintering activity and mixed conductivity will be improved if a transition metal ion, the valence of which is lower than 4+, is doped into ceria to form a solid solution [17]. Zhang et al. [18] reported that manganese-doped ceria (MDC) exhibited a beneficial capability of sintering and densification. Kang et al. [17] indicated that MDC was a potential mix conductor in oxygen atmosphere. However, MDC materials have not been studied as SOFC anode.

In this paper, the manganese-doped ceria powder was synthesized, and its various properties were studied. We expect that the improvement of sintering activity by Mn-doping would help getting a stronger combination of anode/electrolyte; meanwhile, the increase in conductivity would help to enhance the anodic activity. Since ceria anodes exhibit volume expansion upon reduction [19], it may decrease the electrochemical performance and stability of the fuel cells [20]. A 30 wt.% ScSZ powder was added to MDC to form a MDC–ScSZ composite anode in order to improve the anode/ScSZ combination and match the thermal expansion further.

G. Cai · R. Liu · C. Zhao · J. Li · S. Wang (✉) · T. Wen
CAS Key Laboratory of Materials for Energy Conversion, Shanghai Inorganic Energy Materials and Power Source Engineering Center, Shanghai Institute of Ceramics, Chinese Academy of Sciences (SICCAS), 1295 Dingxi Road, Shanghai 200050, People's Republic of China
e-mail: srwang@mail.sic.ac.cn

Experimental procedure

Powder and sample preparation

Different molar ratios of MDC powders were synthesized via citric acid nitrate method. The start materials were $MnCO_3$ (99%, Sinopharm Chemical Regant Co. Ltd.) and $Ce(NO_3)_3{\cdot}5H_2O$ (99.5%, Rare-Chem Hi-Tech Co. Ltd.). These start materials were directly mixed in a nitrate solution with different molar ratios of Ce/Mn (CeO_2/MnO_2 were 10:0, 9:1, 8:2, and 7:3, respectively). In addition, citric acid (99.5%, Shanghai Chem. Ltd., China) was added into the mixture, and the molar ratio of metal ions to citric acid was 1:1.5. As soon as the mixture completely became gel, it was heated at 180 °C for 48 h in order to obtain the precursor of the synthesized powder. Afterward, the precursor was calcined at 800 °C for 4 h in air. After these steps, the synthesized powders were marked as CeO_2, MDC10, MDC20, and MDC30 (0, 10, 20, and 30 mol.% Mn-doping, respectively). X-ray diffraction analysis (Rigaku D/max 2550V) with Cu K_α radiation and Ni filter was used to identify the phase of these synthesized powders and study the chemical compatibility of MDC with ScSZ [$(ZrO_2)_{0.89}(Sc_2O_3)_{0.1}(CeO_2)_{0.01}$, Tosoh, Japan]. The MDC/ScSZ powders were mixed at a 1:1 weight ratio and then calcined at 1250 °C for 3 h in air.

For conductivity, sintering shrinkage and thermal expansion coefficients (TEC) measurements, MDC and CeO_2 powders were die-pressed into the 5 mm diameter and 15 mm high cylinder samples at 300 MPa. Then, the MDC samples were sintered at 1350 °C for 4 h in air, while the CeO_2 sample was sintered at 1500 °C. The densities of the samples were measured by Archimedes method. The TEC and sintering shrinkage were measured by NETZSCH DIL 402PC with a heating rate of 5 °C min^{-1}. The conductivity was measured by standard four-probe method in humidified hydrogen (with 3% H_2O) from 500 to 900 °C. The samples were firstly reduced in H_2 at 900 °C for almost 12 h to ensure that the dense samples were fully reduced.

Fuel cell preparation

To prepare fuel cells, the mixture of 30 wt% ScSZ and 70 wt.% $La_{0.8}Sr_{0.2}MnO_3$ (LSM) was used as cathode and coated on a 170 μm dense ScSZ electrolyte substrate by screen printing, then followed by calcined at 1200 °C for 3 h. MDC–ScSZ slurry was prepared by mixing the MDC–ScSZ (70:30 wt) with terpilenol and ethyl cellulose. The slurry was screen printed on the electrolyte substrate, then followed by calcination at 1150 °C for 3 h. Au and Pt pastes were used as current collector for anode and cathode sides, respectively. Each cell with the cathode area of 1.33 cm^2 was sealed onto alumina tubes via glass ring. The entire cell was placed inside a furnace and heated to 900 °C. Meanwhile, H_2 or CH_4 with 3% H_2O was introduced to the anode side with a flow rate of 25 and 15 mL min^{-1}, respectively. O_2 was introduced to the cathode side with a flow rate of 25 mL min^{-1}. Before the fuel cell tests, the anode was reduced in H_2 at 900 °C for 5 h. The current–voltage curves and electrochemical impedance spectroscopy were obtained by IM6e-X (ZAHNER, Germany) with 20 mV amplitude over the frequency range of 0.03 Hz to 100 kHz. The fuel cell was tested in H_2 or CH_4. The microstructures of the cells after tests were examined with scanning electron microscope (SEM) by an electron probe micro analyzer (EPMA, JXA-8100, JEOL).

Results and discussion

Characterization of MDC powders

As shown in Fig. 1, MDC powders calcined at 1350 °C exhibited single fluorite phase compared with the standard XRD pattern of CeO_2 (JCPDS card no. 34-0394). However, little by-product Mn_3O_4 (JCPDS card no. 24-0734) were observed in MDC30 patterns. The MDC–ScSZ composite remained its original phase peaks, which indicated that there was not any severe reaction between MDC and ScSZ under 1250 °C. Hence, the MDC material had a beneficial compatibility with ScSZ.

The linear shrinkages ($\Delta L/L_0$) of CeO_2 and MDC samples sintered at a constant heating rate of 5 °C min^{-1} from room temperature to 1350 °C were shown in Fig. 2. At 1350 °C, the shrinkage ($\Delta L/L_0$) of MDC10, MDC20, and MDC30 are 19%, 18%, and 24%, respectively, while the one of CeO_2 was only 8%. The Mn-doping increased

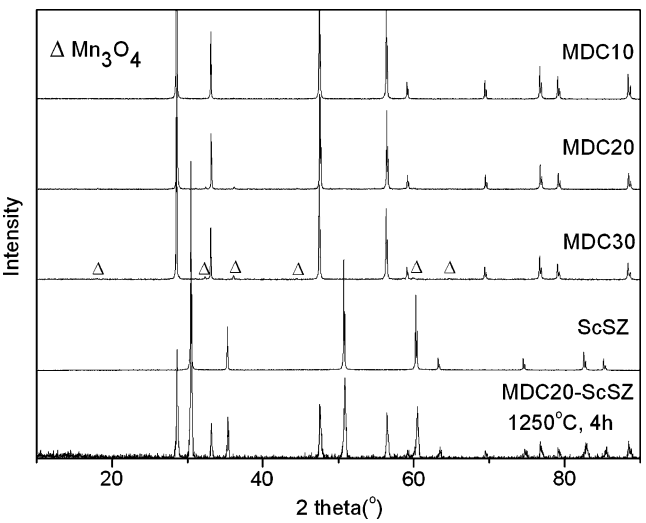

Fig. 1 XRD patterns of MDC10/20/30 calcined at 1350 °C, MDC20–ScSZ composite calcined at 1250 °C

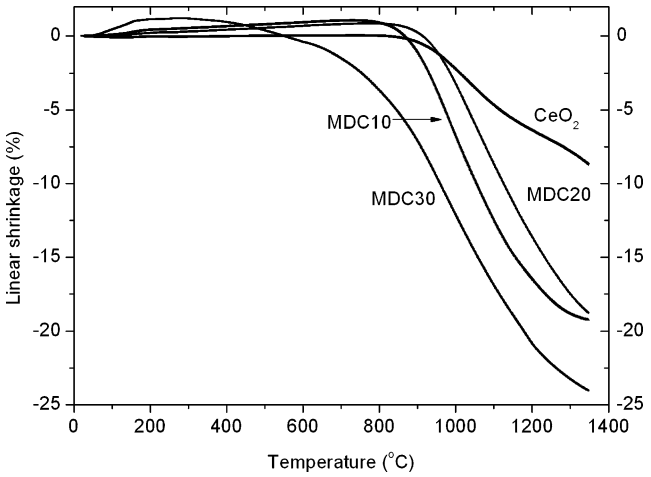

Fig. 2 Linear shrinkage versus sintering temperature for CeO_2, MDC10, MDC20, and MDC30 sintered at a heating rate of 5 °C min^{-1}

the total sintering shrinkage of the samples. These results suggested that Mn-doping can dramatically reduce the sintering temperature of CeO_2 [21], which was good for the fuel cells to obtain a strong combination of anode/electrolyte.

Characterization of MDC samples

In this work, we studied the conductivities of MDC10, MDC20, MDC30, and CeO_2 samples in reducing atmosphere, which were shown in Fig. 3. The relative densities of these samples were 98% (MDC10), 96% (MDC20), 97% (MDC30), and 94% (CeO_2). In Fig. 3, the MDC10 sample exhibited the highest conductivity. At 900 °C, the conductivities of MDC10, MDC20, MDC30, and CeO_2 were 4.12, 2.70, 1.19, and 1.94 Scm^{-1}, respectively. The conductivity CeO_2 was lower than that of MDC20 sample yet higher than the MDC30 one. The results indicated that appropriate Mn doping can enhance the conductivity of CeO_2 in reducing atmosphere.

Figure 4 showed the thermal expansion curves of MDC and ScSZ in air. Further calculation indicated that the average thermal expansion coefficients (TEC) of ScSZ, MDC10, MDC20, and MDC30 between 20 and 900 °C were 10.64×10^{-6}, 11.95×10^{-6}, 12.72×10^{-6}, and $13.22\times10^{-6}K^{-1}$, respectively. The MDC10 sample matched best with the ScSZ that was good for maintaining long-term stability and enduring thermal cycle.

SEM observation

Figure 5 showed the cross-section SEM images of tested fuel cells using MDC10–ScSZ (cell 1), MDC20–ScSZ (cell 2), and CeO_2-ScSZ (cell 3) as anodes. The thickness of dense ScSZ electrolyte, anode, and cathode were about 170, 50, and 20 μm, respectively. Meanwhile, the microstructure of the MDC10–ScSZ anode was fine, continuous, and had uniform micropores. In Fig. 5b, the larger grains with an average grain size of 1–2 μm were ScSZ grains, which conduct oxygen ions. The smaller grains with an average grain size of 0.5–1 μm were MDC grains, which were electron and ions conductors. The micropores, ScSZ grains, and the MDC grains constitute a triple phase boundary. We noticed that cell 1 presented the best anode/electrolyte interface because that of MDC10 exhibited the best sintering activity and match the TEC of ScSZ best. This was beneficial for obtaining high performance and stable long-term operation.

Performance of single cells

The performances of fuel cells in H_2 at 900 °C were shown in Fig. 6. With the Mn doping in CeO_2, the maximum

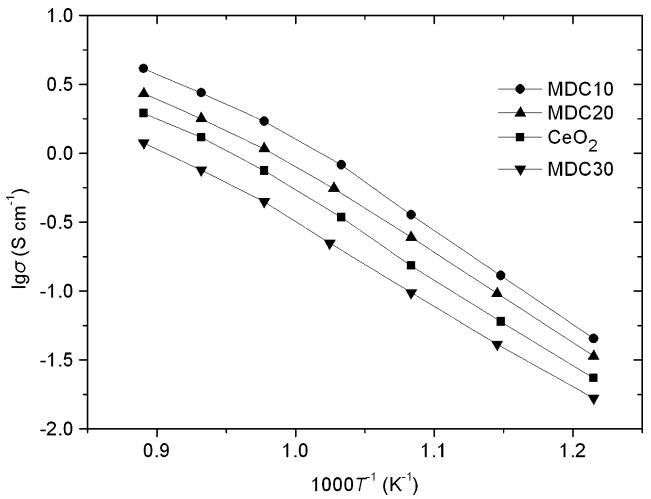

Fig. 3 Electrical conductivity of MDC10/20/30 and CeO_2 at various temperatures in reducing atmosphere

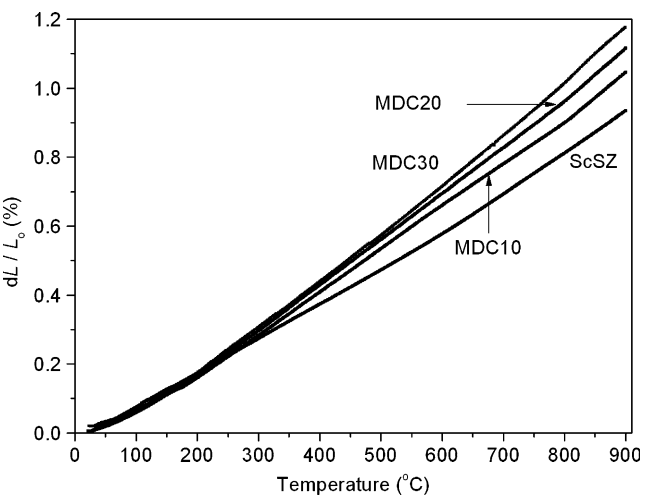

Fig. 4 Thermal expansion curves of ScSZ, MDC10, MDC20, and MDC30 in air

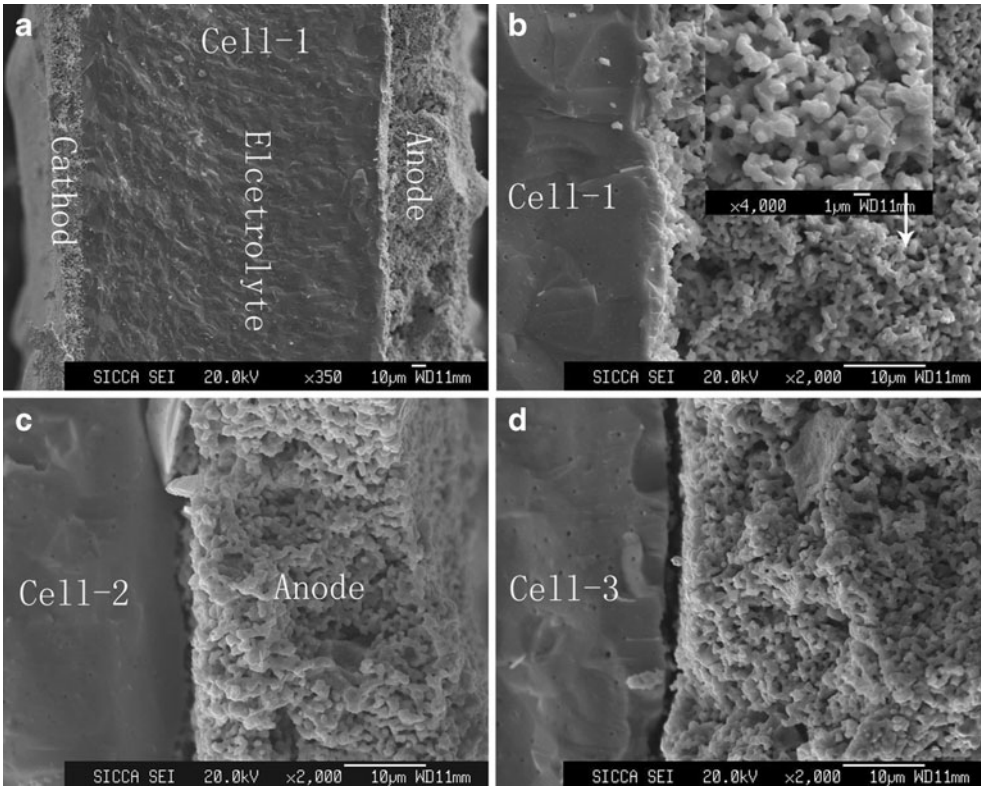

Fig. 5 SEM images of **a** MDC10–ScSZ anode with ScSZ electrolyte and LSM20–ScSZ cathode, **b** the interface of MDC10–ScSZ anode and ScSZ electrolyte, **c** the interface of MDC20–ScSZ anode and ScSZ electrolyte, **d** the interface of CeO_2–ScSZ anode and ScSZ electrolyte

power density (MPD) improved significantly; the MPD at 900 °C increased from 166 to 318 mW cm^{-2}. The MPDs of cells 1 and 2 were 318 and 204 mW cm^{-2}, which were acceptable performances. These results were agreed with the conductivity measurements above. Figure 7 showed the curves of voltage and power density versus current density, while the fuel cell was running on 3% H_2O saturated CH_4. Cell 1 exhibited a better performance than cell 2 in CH_4, and the MPD of cells 1 and 2 were 262 and 179 mW cm^{-2} at 900 °C. Fuel cells in CH_4 remained about 80% performances of those in H_2. These results showed that the MDC10–ScSZ composites were potential candidates for SOFCs anode in hydrocarbon fuels.

In an attempt to examine the different performances of the fuel cells, we measured the impedance spectra of fuel cells on H_2 and CH_4 as displayed in Figs. 8 and 9, respectively. The low frequency intercept corresponded to the total resistance of the cell. The high frequency intercept represented the ohmic resistance (R_o), involving ionic resistance of the electrolyte, electronic resistance of the electrodes, and some contact resistance associated with interfaces [22]. In Fig. 8, the R_O values were 0.279, 0.476,

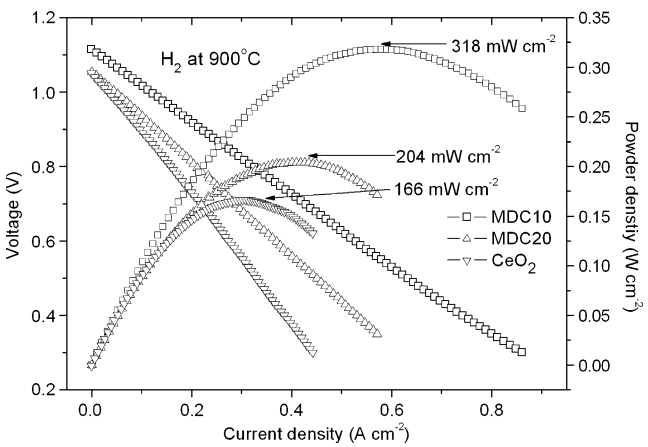

Fig. 6 Electrochemical performance of single fuel cells operating in H_2+3% H_2O at 900 °C

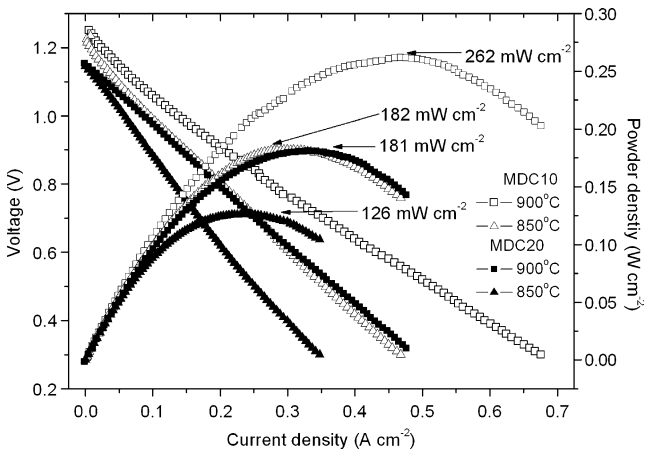

Fig. 7 Electrochemical performance of single fuel cells operating in CH_4+3% H_2O

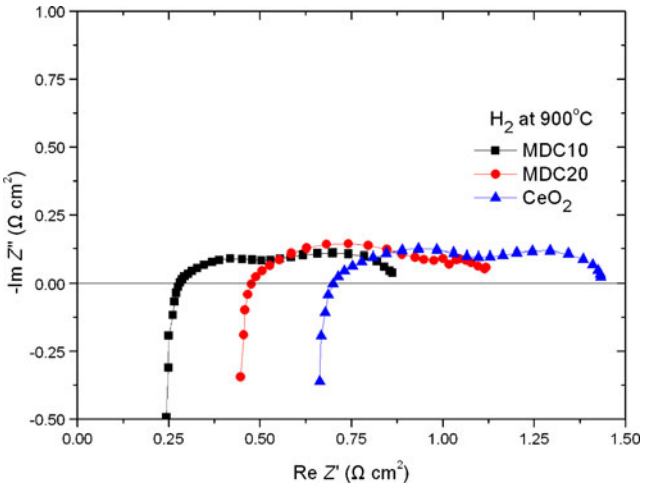

Fig. 8 Electrochemical impedance spectroscopy under open circuit conditions of the fuel cells operating in H_2+3% H_2O at 900 °C

and 0.702 Ωcm^2 for MDC10–ScSZ, MDC20–ScSZ, and CeO_2–ScSZ, respectively. It demonstrated that the improvement of fuel cell performance was partly due to the change of R_O. Since the electrolyte and cathode of the fuel cells were the same, the increases in power density were mainly contributed from the different anodes. MDC10–ScSZ anode presented a higher conductivity and lower R_O of electrodes/electrolyte interface. The difference between the high frequency and low frequency intercepts represents the electrode polarization resistance (R_P), which corresponded to mass transport process. The R_P values were 0.583, 0.635, and 0.739 Ωcm^2 for MDC10–ScSZ, MDC20–ScSZ and CeO_2–ScSZ, respectively. The decrease of R_P from MDC10/20 to CeO_2 showed that the Mn doping brought a stronger interfacial combination between anode and electrolyte, leading to extend the efficient active area of fuel cells. In Fig. 9, the R_P values at 900 °C were 0.727 and

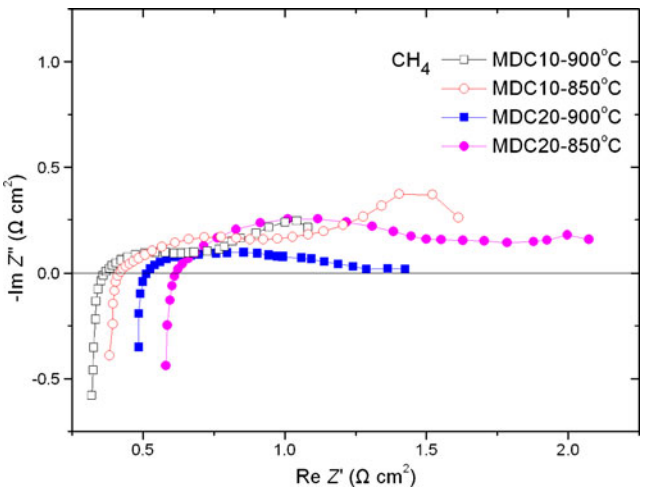

Fig. 9 Electrochemical impedance spectroscopy under open circuit conditions of the fuel cells operating in CH_4+3% H_2O

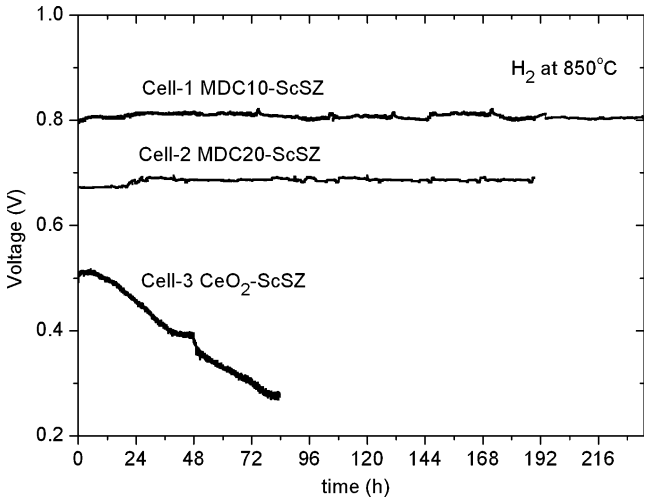

Fig. 10 The voltages change of the cells with MDC10–ScSZ, MDC20–ScSZ, and CeO_2–ScSZ anodes during a long duration discharge at a current density of 200 mA cm^{-2} at 850 °C in H_2+3% H_2O

0.891 Ωcm^2 for MDC10–ScSZ and MDC20–ScSZ, which were higher than those in H_2.

Figure 10 showed the voltages change of the cells during a long duration discharged at a current density of 0.2 Acm^{-2} at 850 °C in H_2 with 3% H_2O. We found that the voltages of the cells 1 and 2 almost remained constant with a little increase with time in the period of 200 h. However, cell 3 performed poor in long-term running, its voltage decreased significantly in 80 h, and some parts of the anode fell off from the electrolyte substrate after the test. The SEM image in Fig. 5d shows why the performnce of cell 3 decreased significantly. In sum, cells 1 and 2 have the potential of operating stably in the long-term running.

Conclusion

Ten and 20% Mn-doped CeO_2 had been synthesized with single fluorite phase, and they were compatable well with the ScSZ electrolyte. MDC powder exibited a favorable sintering activity, and it can be densified at 1350 °C. The conductivity of MDC10/20 was higher than that of CeO_2; for example, the conductivities of MDC10, MDC20, and CeO_2 were 4.12, 2.70, and 1.94 Scm^{-1} at 900 °C. The TEC measurements indicated that MDC10/20 anode matched with the ScSZ electrolyte. The performances of fuel cell with MDC10/20–ScSZ as anodes in H_2 and CH_4 have been evaluated. When the fuel cells used Mn-doped CeO_2 as anode instead of CeO_2, the R_O and R_P decreased, together with the maximum power density increased. The cell with MDC10–ScSZ as anode presented maximum power densities of 318 and 262 mW cm^{-2} in H_2 and CH_4, respectively. The results demonstrate that MDC10–ScSZ composites can be considered as a potential candidate of SOFCs anode.

Acknowledgements The authors thank the financial support from Chinese Government High Tech Developing Project

References

1. Singhal SC (2002) Solid State Ionics 152–153:405–410
2. Gorte RJ, Kim H, Vohs JM (2002) J Power Sources 106:10–15
3. Jiang SP, Chan SH (2004) Mater Sci Technol 20:1109–1118
4. Jiang SP, Chan SH (2004) Mater Sci 39:4405–4439
5. Bartholomew CH (1982) Catal Rev Sci Eng 24:67–70
6. Baker RTK (1989) Carbon 27:315–323
7. Steele BCH (1996) Solid State Ionics 86–88:1223–1234
8. Hernadi K, Fonseca A, Nagy JB, Siska A, Kiricsi I (2000) Appl Catal A199:245–255
9. Koh JH, Yoo YS, Park JW, Lim HC (2002) Solid State Ionics 149:157–166
10. Farrauto RJ, Batholomew CH (1997) Fundamentals of industrial catalytic processes, 1st edn. Blackie Academic & Professional, London, pp 341–343
11. Marina OA, Mogensen M (1999) Appl Catal A189:117–126
12. Ye XF, Huang B, Wang SR, Wang ZR, Xiong L, Wen TL (2007) J Power Sources 164:203–209
13. An S, Lu C, Worrell WL, Gorte RJ, Vohs JM (2004) Solid State Ionics 175:135–138
14. Zhan ZL, Barnett SA (2005) Science 308:844–847
15. Sun CW, Sun J, Xiao GL, Zhang HR, Qiu XP, Li H, Chen LQ (2006) J Phys Chem B 110:13445–13452
16. Skorodumova NV, Simak SI, Lundqvist BI, Abrikosov IA, Johansson B (2002) Phys Rev Lett 89:166601(1)–166601(4)
17. Kang CHY, Kusaba H, Yahiro H, Sasaki K, Teraoka Y (2006) Solid State Ionics 177:1799–1802
18. Zhang TS, Hing P, Huang H, Kilner J (2001) Mater Sci Eng B 83:235–241
19. Mogensen M, Lindegaard T, Hansen UR, Mogensen G (1994) J Electrochem Soc 141:2122–2128
20. Ahn K, He HP, Vohs JM, Gorte RJ (2005) Electrochem Solid-State Lett 8:A414–A417
21. Panhans MA, Blumenthal RN (1993) Solid State Ionics 60 (4):279–298
22. Xia C, Liu M (2002) Adv Mater 14:521–523